

Improved sliding wear-resistance of alumina with sub-micron grain size: A comparison with coarser grained material

R. Singha Roy^a, H. Guchhait^b, A. Chanda^b, D. Basu^{a,*}, M.K. Mitra^b

^a Central Glass Ceramic Research Institute, Kolkata 700032, India

^b Jadavpur University, Kolkata 700032, India

Received 26 November 2006; received in revised form 12 February 2007; accepted 18 February 2007

Available online 18 April 2007

Abstract

Un-lubricated sliding wear behaviour of sub-micron grained (average grain size, $G = 0.45 \mu\text{m}$), self-mated alumina was studied using conformal-contact with a unidirectional pin-on-disc wear testing machine. The wear characteristics of higher grained alumina samples ($G = 0.95$ and $4 \mu\text{m}$) are also studied under self mating condition for comparative analysis by using similar test parameters and identical test configuration. Sub-micron grained alumina exhibits substantially higher wear resistance compared to the alumina of larger grain size. Scanning electron microscopy of the worn out test samples reveals that in un-lubricated condition, compaction of wear debris on sliding surface governs the wear characteristics of the present set of alumina. In many cases, partly revealed intergranular fracture was noticed. The strength of adhesion of the compacted wear debris with sliding surface increases with decreasing grain size. In case of alumina of larger grain size, the stability of the compacted layer decreases due to cracking. For sub-micron grained alumina, compacted layer of debris with increased adherence efficiently protects the virgin material resulting substantial decrease in wear loss.

© 2007 Elsevier Ltd. All rights reserved.

Keywords: Grain size; Wear resistance; Al_2O_3 ; Wear debris

1. Introduction

Significant improvement in mechanical properties of alumina is possible through refinement of grain size. Particularly, in recent time, with the growing availability of nano-sized commercial powders, researchers have successfully fabricated sub-micron grained alumina with high strength,¹ high hardness^{2,3} and moderately high toughness.⁴ These favourable properties make this new generation, fine-grained alumina an attractive material for load bearing and wear resistant applications ranging from pump, seals, nozzles to high-precision biomedical-implants. Different novel processing routes such as hot iso-static pressing (HIP),⁵ pressure filtration or gel casting^{1,6,7} were employed for this purpose. Even the age old slip casting technique has also been exploited to produce sub-micron grained alumina with the help of well-dispersed agglomerate-free slip.⁸

It has been already reported that a reduced grain size and a narrow grain size distribution often promote improved sliding and abrasive wear resistance of alumina.^{9–11} On the contrary, in some cases, it has also been observed that increase in grain size leads to increased wear resistance properties.^{12–14} Surprisingly, almost in all the above-mentioned studies, grain sizes involved were in the order of one micron or more. In 1996, Krell et al.¹¹ first reported wear characteristics of sub-micron grained alumina ($G \sim 0.5 \mu\text{m}$) at different humidity levels using fretting wear-test configuration. Recently, Singha Roy et al.¹⁵ have described wear behaviour of $0.45 \mu\text{m}$ grained alumina in biological environment. However, regarding un-lubricated sliding wear behaviour of this new grade of high purity sub-micron grained alumina, no further work has been reported till date and consequently understanding about the wear mechanisms of alumina with newly available sub-micron grain size still remains far from being complete. In the present work, un-lubricated sliding wear behaviour of alumina with sub-micron grain size (average grain size = $0.45 \mu\text{m}$) has been investigated. The result is compared with the wear characteristics of similar material with higher grain size (0.95 and $4 \mu\text{m}$) under identical test-conditions.

* Corresponding author. Tel.: +91 33 2473 3469/96; fax: +91 33 2473 0957.
E-mail address: dbasu@cgcrici.res.in (D. Basu).

2. Materials and method

Sub-micron grained alumina was prepared by slip casting⁸ of commercially available α -alumina powder (TM DAR, Taimei Chemical Co., Japan, Purity: 99.99%) with a mean particle size of 170 nm. No sintering aid was added in the as-such procured powder. The powder was dispersed in water with an additive of HCl. The pH of the solution was optimized by a series of sedimentation experiments and kept constant at a value of 2.4. A solid loading of 30-vol.% was used to prepare the samples. Soft agglomerates were broken by ultrasonic agitation and the pH value was kept constant throughout the process by adding additional HCl whenever required. The slip was kept unstirred for 24 h to allow the hard agglomerates to settle down which were then eliminated by carefully separating the supernatant. The slip was poured in a gypsum mould and the cast samples were air-dried. The air-dried samples were then further dried up to 120 °C in an air-oven by increasing the temperature at a rate of 10 °C/day and subsequently pre-fired at 800 °C for 1 h to obtain a pre-fired density of >64% of the theoretical density. Pre-fired samples were carefully ground to the shape of rectangular bar and then sintered at 1275 °C for 1 h to obtain a relative density of >99.8%. One end of the sintered bars were mounted in an araldite-based polymer and subsequently given to a shape of cylinder of 3.25 mm diameter with the help of a cylindrical grinding machine. A 45° bevelled cut at the tip of

the pin was made by using a surface-grinding machine. Finally the flat surface of the cylindrical pin samples were polished to a roughness value of $R_a < 0.05 \mu\text{m}$. The disc ($\phi = 150 \text{ mm}$, thickness = 8.5 mm) with a central hole of 25 mm was also prepared through identical processing steps.

The microstructure (Fig. 1(a)) of the polished and thermally etched samples was obtained by using a scanning electron microscope (LEO 430i STEROSCAN, UK). The grain sizes were determined by linear interception: average grain size $G = 1.56 \times \text{average linear intercept}$ ¹⁶ and was found to be $G = 0.45 \mu\text{m}$. Wear test samples of coarser grain sizes (0.95 and 4 μm) were prepared by cold iso-static pressing (=150 MPa) of the alumina powder followed by sintering at 1350 and 1600 °C, respectively (Fig. 1(b and c)) and for comparison, they were also used in the present wear study. Vicker's hardness and fracture toughness¹⁷ of all the sintered samples were determined by indentation on polished sample ($\approx 16.5 \text{ mm}$ diameter \times 2.2 mm thickness) at 50 N load.

Simple pin-on-disc unidirectional wear and friction testing machine (model no. TR 20L manufactured by M/s Ducom, Bangalore, India) was used for this study. Each pin sample was ultrasonically cleaned and dried before and after the experiment. Volumetric wear of pin was calculated from gravimetric measurement. All the experiments were conducted with a sliding speed of 0.2 m/s under a constant rotational speed of 50 rpm of the disc. The temperature and relative humidity of the room

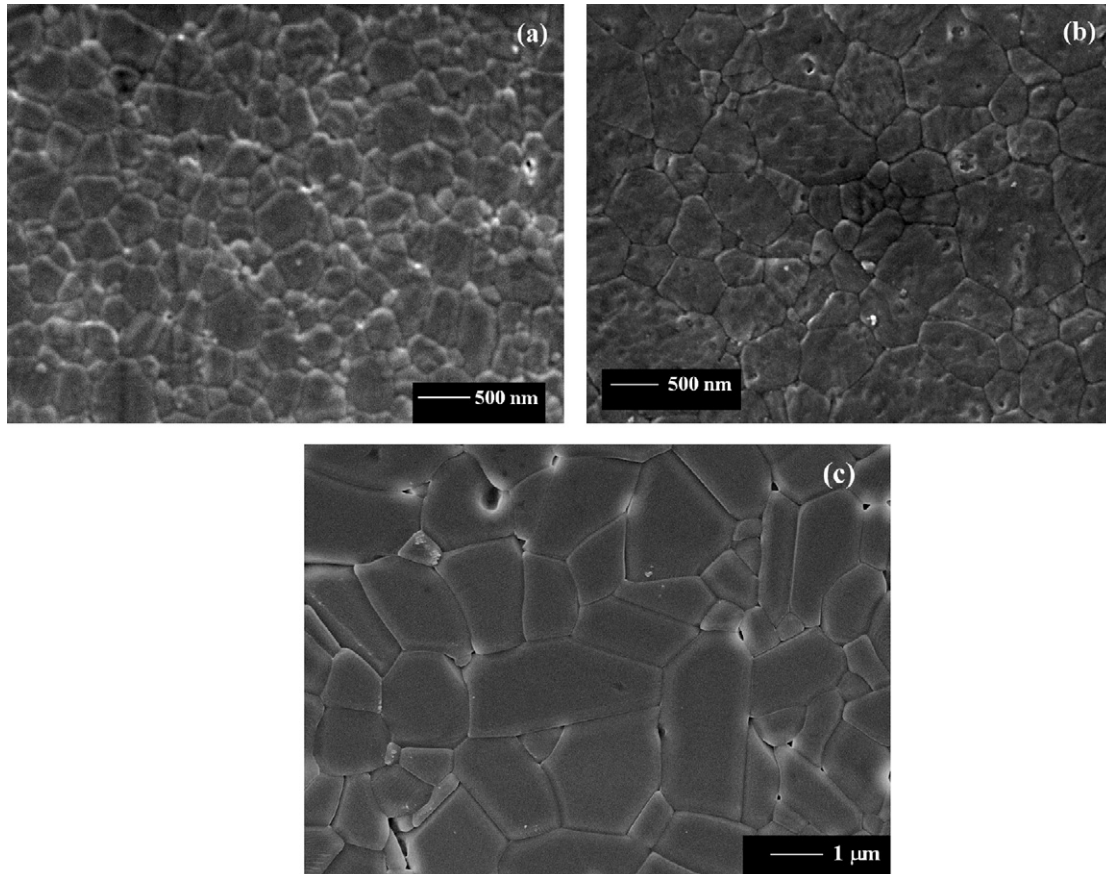


Fig. 1. Microstructure of the alumina used for the present study with average grain size of (a) $G = 0.45 \mu\text{m}$, (b) $G = 0.95 \mu\text{m}$ and (c) $G = 4 \mu\text{m}$.

was kept constant at 24 °C and 45%, respectively. Each test was continued up to a sliding distance of 7.2 km with normal load of 50 N. The samples were weighed before and after the test on an electronic microbalance (METTLER TOLEDO, model no. AG 285) with an accuracy up to five decimal places. Each experiment was repeated at least thrice to check the reproducibility of data. The wear rate of the worn out samples were calculated by using the following equation:

$$\text{wear rate} = \frac{\text{volume loss due to wear}}{\text{normal load} \times \text{sliding distance}}$$

3. Results

The density, Vicker's hardness and indentation fracture toughness of the alumina used in the present study are shown in Table 1. The average coefficient of friction (μ) of three different varieties of alumina and their nature of variation with sliding distance are presented in Fig. 2(a and b). In case of coarser alumina, i.e. $G = 0.95$ and $4 \mu\text{m}$, up to a sliding distance of ~ 2.35 km, ' μ ' was found to be high with substantial fluctuations, which gradually decreased to a stable value (Fig. 2(a)). This initial instability or the transient response may be treated as the start-up period. It was interesting to observe that the sub-micron grained alumina

Table 1

Density, Vickers hardness and indentation fracture toughness (test load = 50 N) data of various grained alumina used in the present study

Grain size	4 μm	0.95 μm	0.45 μm
Density (g/cm^3)	3.94	3.92	3.96
Vickers hardness (GPa)	17.50	20.56	23.77
Indentation toughness ($\text{MPa m}^{0.5}$)	3.21	3.25	3.28

exhibits almost no start-up period during wear experiments and the probable reasons for this are discussed later. For sub-micron grained alumina, at the beginning of the test, ' μ ' shows a slightly lower value which then slowly increases and ultimately secures stability.

Wear resistance of the sub-micron alumina was found to be substantially high (Fig. 2(c)). The average value of wear rate was found to decrease with decreasing average grain size and sub-micron grained alumina with $G = 0.45 \mu\text{m}$ suffered minimum wear. The value was ~ 5 – 6 times lower than that in case of alumina with higher grain sizes.

SEM micrographs of the worn out pin samples show that the compaction of wear debris on sliding surfaces occurs in sub-micron grained alumina (Fig. 3). In higher grained alumina too, compaction was frequently noticed (Figs. 4 and 5). The

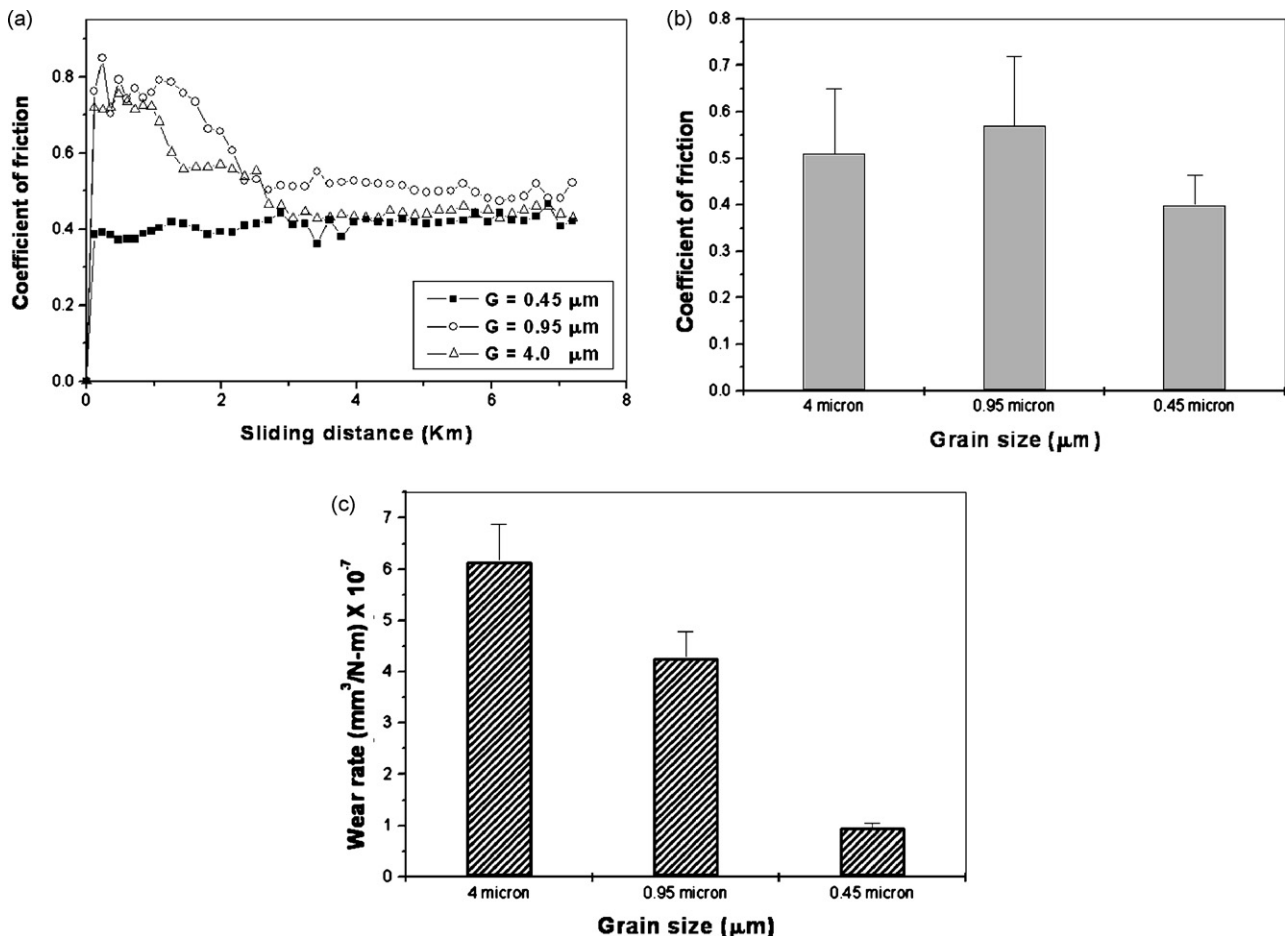


Fig. 2. (a) Variation in coefficient of friction with sliding distance, (b) average coefficient of friction and (c) average wear factor of various alumina used in the present study.

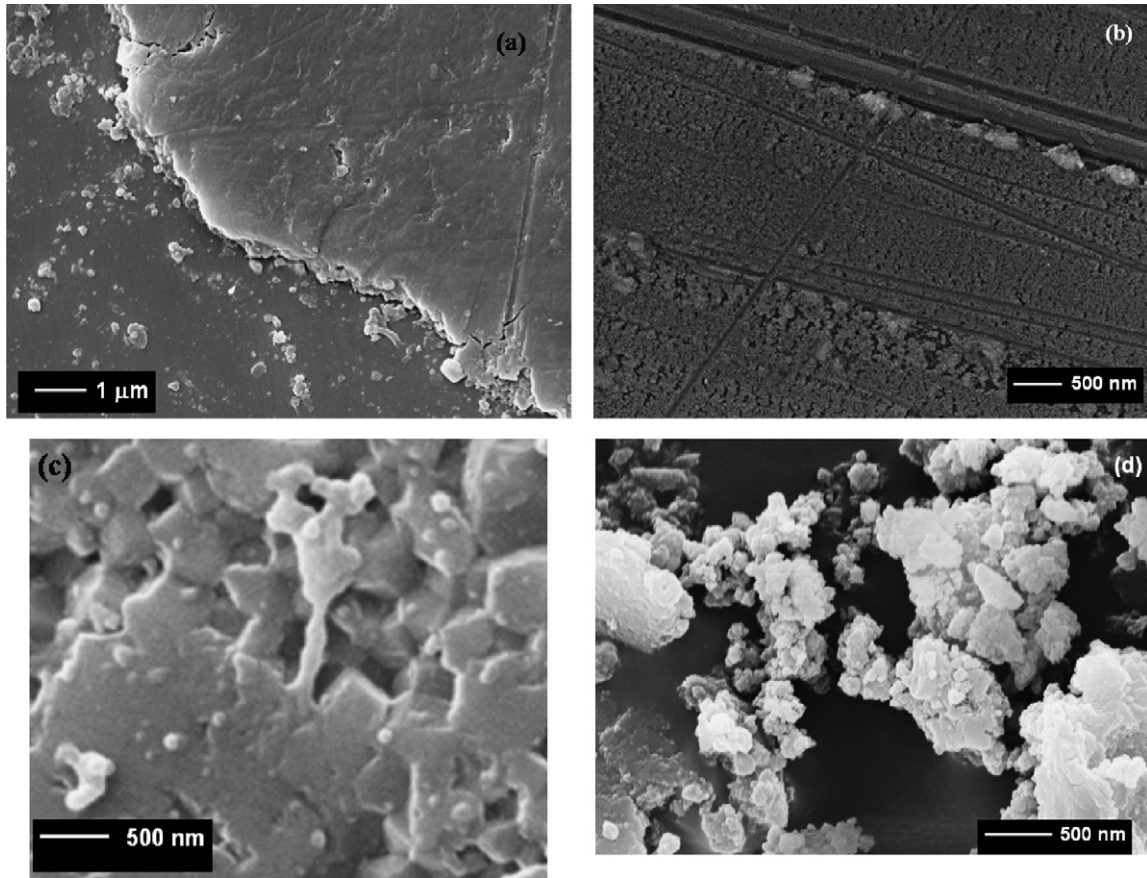


Fig. 3. SEM micrograph for worn-out alumina pin with $0.45\ \mu\text{m}$ grain size, showing (a) layer of compacted wear debris on the sliding surface of sub-micron alumina, (b) ploughing marks on the compacted layer, (c) intergranular fracture partially covered by compacted wear debris and (d) wear debris generated due to friction of sub-micron alumina.

SEM analysis of the wear debris generated in the present study shows that the morphology of wear debris (collected on adhesive tape) generated from all the alumina specimens, is more or less same and their size lies in the range of 20–50 nm; however, in most of the cases, they exist in the form of lump or agglomerate (Fig. 3(d)). In all the cases, the compacted layer was produced by these fine particles, generated by repeated fragmentation of the dislodged grains which thereafter formed agglomerates, got

compressed and during further sliding, plastically deformed into layers (Figs. 3(a), 5(a)). For higher grained alumina (i.e. $G = 4$ and $0.95\ \mu\text{m}$), significant amount of cracking in the compacted surface layer was observed and in many cases, this resulted to the development of fish-scale like surface features by forming a network of micro-cracks (Fig. 5(a)). However, for the sub-micron grained sample, fair amount of scratching or ploughing marks were observed on the compacted layer (Fig. 3(a and b)).

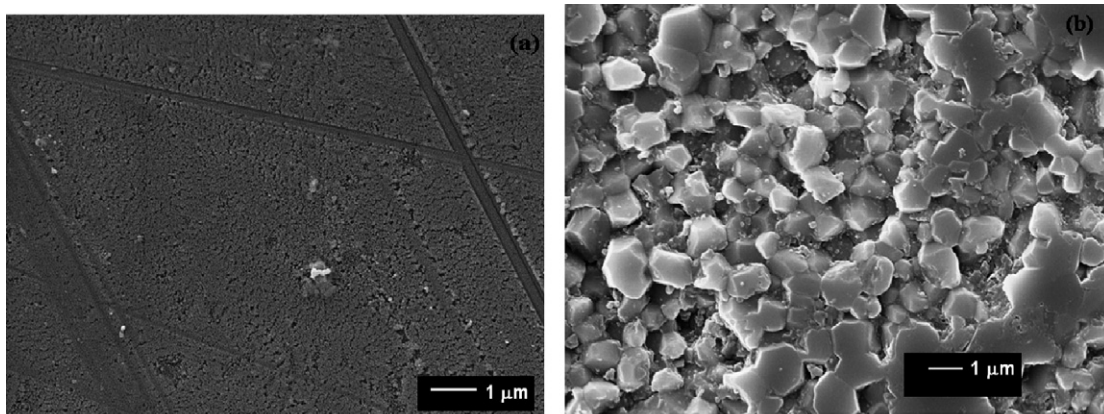


Fig. 4. SEM micrographs for worn-out alumina pin with $0.95\ \mu\text{m}$ grain size, showing (a) abrasion marks on the compacted layer of wear debris and (b) intergranular fracture with evidences of grain boundary microcracking.

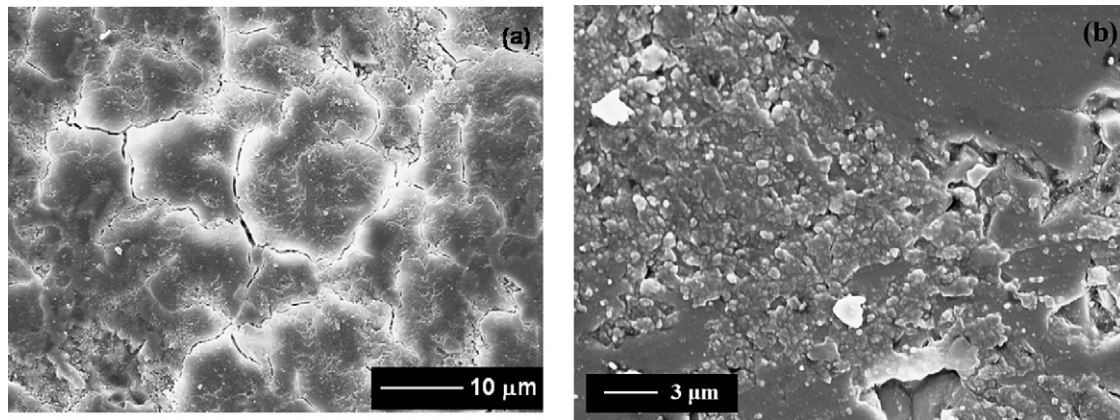


Fig. 5. SEM micrographs for worn-out alumina pin with 4 μm grain size, showing (a) ‘fish-scale’ like structure generated by networking of microcracks in the compacted layer and (b) partly revealed brittle fracture beneath the layer of compacted wear debris.

For alumina with medium grain size (i.e. $G=0.95 \mu\text{m}$), occasional cases of ploughing on the compacted layer were observed (Fig. 4(a)). The SEM study of the worn out alumina pins with $G=0.45 \mu\text{m}$ reveals few areas where inter-granular fracture was noticed (Fig. 3(c)). However, in case of 0.95 and 4 μm grain size, extensive grain pull-out was observed in selected zones (Fig. 4(b)).

4. Discussion

It is evident that for all grain sizes of alumina, wear involves generation of fine particles and their compaction. This compacted layer was found to play key role in the progressive wear events for all the alumina samples under investigation (Figs. 3 and 5). In case of unidirectional wear tests with self mated alumina, several researchers have already reported about the compacted layer containing significant amount of aluminium hydroxide which may exist in the form of either boehmite or bayerite.^{18–20} In this particular study, perhaps the conformal contact between the surfaces enhanced the scope of entrapment and accumulation of fragmented particles. The SEM analysis of the wear debris generated in the present study does not reveal any major difference regarding the shape and size. The size of the debris being very small, in almost all the cases it was found that owing to high surface energy, they formed lumps. With time, these lumps got plastically deformed and caused the formation and progressive development of the layer. It is quite obvious that finer these alumina particles are, greater will be their propensity to react with moisture in the surrounding atmosphere to form such agglomerate or hydroxide surface layer which suffers compaction with time. This surface layer is not only prone to fracture-damage but also much softer and suffers plastic deformation than the remnant alumina particles and influences the wear mechanism.

It was found that for all the alumina pins used in the present study, the compacted and plastically deformed debris covers almost the entire surface. For coarser alumina (i.e. $G=4$ and $0.95 \mu\text{m}$), cracking in the compacted layer formed fish-scale like surface features (Fig. 5(a)). The cracks might have been generated due to the combined action of repeated cyclic and ther-

mal stresses in compacted layer. However, for the sub-micron grained sample, the wear debris strongly adhered to the sub-surface and did not suffer spalling or micro-fracture like other cases. In this case, fair amount of scratching or ploughing marks were observed on the compacted layer (Fig. 3(a and b)), in contrast to occasional cases of ploughing (Fig. 4(a)) for alumina with medium grain size (i.e. $G=0.95 \mu\text{m}$). Generation of similar type of unstable compacted layer with increasing grain size has also been noticed in alumina–alumina wear couples by Zum Gahr et al.²¹ In case of fine-grained material (e.g. $G=0.45 \mu\text{m}$ in the present case), this strongly adherent layer efficiently protects the underneath material and enhances the overall wear resistance. Moreover in such cases, after fragmentation, the grain size becomes even finer which readily reacts with moisture to form aluminium hydroxide and gets accumulated at different surface pores and discontinuities resulting the sliding surfaces smooth and soft. This results in low coefficient of friction with minimum fluctuations in case of smallest grain size in contrast to higher grained alumina i.e. $G=0.95$ and $4 \mu\text{m}$, where fair amount of scatter in coefficient of friction values during initial start-up period was observed (Fig. 2(a)).

As mentioned earlier, the SEM study of the worn out alumina pins with $G=0.45 \mu\text{m}$ reveals few areas where intergranular fracture was noticed (Fig. 3(c)) while, in case of 0.95 and 4 μm grain size, extensive grain pull-out was observed (Fig. 4(b)). This is in accordance with the proposition of Ajayi and Ludema²² regarding wear of alumina by grain boundary microfracture. As intergranular microfracture and grain dislodgement occurs through microcrack propagation along individual grain boundaries, instead of long crack toughness, grain boundary toughness becomes guiding factor for wear loss in such situation. Wear-damage-induced stress (σ_D) required to produce such grain boundary micro-fracture are calculated by using the following relationship (Eq. (1))⁹ and shown in Table 2

$$\sigma_D = \sigma_I \left[\left(\frac{l}{l_*} \right)^{-1/2} - 1 \right] \quad (1)$$

where σ_I is the internal tensile stress due to thermal expansion anisotropy, the maximum value of σ_I can be =100 MPa,

Table 2
Wear-damage-induced stress required to cause grain boundary micro-fracture for different grain sizes of alumina used in the present study

Grain size, l (μm)	Wear damage stress, σ_D (MPa)	
	Cho et al. ⁹	Krell et al. ²⁶
4	900	450
0.95	1952	570
0.45	2881	633

l the grain size of the alumina used in the experiment, $l^* = 400$ MPa, the critical grain size limit of alumina for spontaneous microfracture due to thermal expansion anisotropy.^{23–25} Following the proposition of Krell et al.²⁶, another set of values of wear-damage-induced stress (σ_D) was calculated (adopting $\sigma_I = 50$ MPa for $4 \mu\text{m}$, 30 MPa for $0.95 \mu\text{m}$ and 22 MPa for $0.45 \mu\text{m}$ from Fig. 5 of the respective reference) and also incorporated in Table 2. However, in the second set of data, the values of σ_D increase towards finer microstructures in a comparatively moderate fashion. Both these set of data indicate that, due to thermal expansion anisotropy, with grain refinement, σ_D increases and makes higher grained alumina more susceptible to grain dislodgement. Hence, grain dislodgement through microcrack propagation and severity of intergranular fracture is higher for coarser grained material. For higher grained material, in many cases, brittle fracture was partly revealed beneath the compacted layer (Fig. 5(b)). In this context, it is to be noted that the formation and subsequent degeneration of compacted layer (either by flake formation or by wear due to continuous sliding motion) is a dynamic process. It may happen that in some portion of the contacting surface, the wear debris is getting compacted and simultaneously in other portions it is being worn out resulting intergranular fracture. Wear, being a system response, is likely to depend on number of intrinsic and extrinsic parameters and therefore number of micro-mechanisms is taking place simultaneously. In the present case too, formation of compacted layer and grain boundary micro-fracture leading to pull-out are likely to occur side by side. Owing to smaller grain size vis-à-vis smaller size of primarily generated wear debris, formation of compacted layer predominated over other mechanism in fine-grained alumina ($G = 0.45 \mu\text{m}$) while in other cases, grain boundary microcracking and intergranular fracture was found to be the main mechanism of wear. So far hierarchy of influences of different material parameters is concerned; combination of hardness (both macro and micro) and fracture toughness comes first. Consequently, variation in wear can be mainly attributed to these governing factors. However, it is apparently evident from the data that there is some sort of variation regarding porosity (higher porosity with higher grain size) that might have contributed as well though it is still a conjecture and requires further detailed experimentation.

5. Conclusions

- Superiority in sliding wear resistance was observed for alumina with $0.45 \mu\text{m}$ grain size.

- Compacted layer of wear debris along with partly revealed brittle fracture on the sliding surface was evident in all cases and with decreasing grain size, extent of adherence of compacted layer increases.
- With progress in wear, owing to subsequent rubbing, compacted layer suffers mild abrasion in smaller grained alumina while for larger grained specimens extensive cracking occurred which led to flaking and delaminations.
- Sub-micron grained samples efficiently protects the underneath material by enhanced adherence with compacted wear debris while in higher grained alumina, cracking followed by flaking damages the protective layer, easily exposes the original sliding surface and leads to significantly high wear loss through intergranular fracture.

Acknowledgements

The authors wish to express their appreciation to Dr. (Mrs.) S. Sen and Mrs. S. Roy for extending their support during SEM study. They would also like to express thanks to Mr. S. Roy, Mr. L.K. Naskar and Mr. H. Mondal for their kind help during sample preparation. Mr. R. Singha Roy wishes to acknowledge CSIR, India for financial support. One of the authors (Dr. A. Chanda) acknowledges financial help from DST, Government of India.

References

1. Krell, A. and Blank, P., The influence of shaping method on the grain size; dependence of strength. *J. Eur. Ceram. Soc.*, 1996, **16**, 1189–1200.
2. Krell, A., Improved hardness and hierarchic influences on wear in sub-micron sintered alumina. *Mater. Sci. Eng. A*, 1996, **209**, 156–163.
3. Krell, A., Grain size dependence of hardness in dense sub-micrometer alumina. *J. Am. Ceram. Soc.*, 1995, **78**, 1118–1120.
4. Mughtar, A. and Lim, L. C., Indentation fracture toughness of high purity sub-micron alumina. *Acta Mater.*, 1998, **46**, 1683–1690.
5. Echeberria, J., Tarazona, J., Heb, J. Y., Butlerb, T. and Castroa, F., Sinter-HIP of α -alumina powders with sub-micron grain sizes. *J. Eur. Ceram. Soc.*, 2002, **22**, 1801–1809.
6. Krell, A. and Ma, H., Nanocorundum—advanced synthesis and processing. *Nanostruct. Mater.*, 1999, **11**, 1141–1153.
7. Krell, A., Blank, P., Ma, H., Hutzler, T. and Nebelung, M., Processing of high-density submicrometer Al_2O_3 for new applications. *J. Am. Ceram. Soc.*, 2003, **86**, 546–553.
8. Lim, L. C., Wong, P. M. and Ma, J., Colloidal processing of sub-micron alumina powder compacts. *J. Mater. Process. Tech.*, 1997, **67**, 137–142.
9. Cho, S.-J., Hockey, B. J., Lawn, B. R. and Benninson, S. J., Grain-size and R -curve effects in the abrasive wear of alumina. *J. Am. Ceram. Soc.*, 1989, **72**, 1249–1252.
10. Mukhopadhyay, A. K. and Mai, Y. W., Grain size effect on abrasive wear mechanisms in alumina ceramics. *Wear*, 1993, **162–164**, 258–268.
11. Krell, A. and Klaffke, D., Effects of grain size and humidity on fretting wear in fine grained alumina, $\text{Al}_2\text{O}_3/\text{TiC}$ and zirconia. *J. Am. Ceram. Soc.*, 1996, **79**, 1139–1146.
12. Xiong, F., Manory, R. R., Ward, L. and Terheci, M., Effect of grain size and test configuration on the wear behaviour of alumina. *J. Am. Ceram. Soc.*, 1997, **80**, 1310–1312.
13. Chaiwan, S., Hoffman, M., Munroe, P. and Stiefel, U., Investigation of sub-surface damage of alumina during wear using focused ion-beam milling. *Wear*, 2002, **252**, 531–539.
14. Terheci, M., Grain boundary and testing procedure, a new approach to the tribology of alumina materials. *Wear*, 1997, **211**, 289–301.

15. Singha Roy, R., Mondal, A., Chanda, A., Basu, D. and Mitra, M. K., Sliding wear behavior of submicron-grained alumina in biological environment (p NA). *J. Biomed. Mater. Res. Part A*, 2007, **83A**, 257–262.
16. Mendelson, M. I., Average grain size in polycrystalline ceramics. *J. Am. Ceram. Soc.*, 1969, **52**, 443–446.
17. Antis, G. R., Chantikul, P., Lawn, B. R. and Marshall, D. B., A critical evaluation of indentation techniques for measuring fracture toughness. I. Direct crack measurement. *J. Am. Ceram. Soc.*, 1981, **64**, 533–538.
18. Gates, R. S., Hsu, S. M. and Klaus, E. E., Tribochemical mechanism of alumina with water. *Tribol. Trans.*, 1989, **32**, 357–363.
19. Gee, M. G., The formation of aluminium hydroxide in the sliding wear of alumina. *Wear*, 1992, **153**, 201–227.
20. Gee, M. G. and Jennett, N. M., High-resolution characterization of tribochemical films on alumina. *Wear*, 1995, **193**, 133–145.
21. Zum Gahr, K.-H., Bundschuh, W. and Zimmerlin, B., Effect of grain size on friction and sliding wear of oxide ceramics. *Wear*, 1993, **162–164**, 269–279.
22. Ajayi, O. O. and Ludema, K. C., Surface damage of structural ceramics: implications for wear modeling. *Wear*, 1988, **124**, 237–257.
23. Blendell, J. E. and Coble, R. L., Measurement of stress due to thermal expansion anisotropy in Al_2O_3 . *J. Am. Ceram. Soc.*, 1982, **65**, 174–178.
24. Lange, F. F., Fracture mechanics and microstructural design. In *Fracture Mechanics of Ceramics*, vol. 4, ed. R. C. Bradt, D. P. H. Hasselman and F. F. Lange. Plenum, New York, 1978, pp. 799–819.
25. Rice, R. W., Pohanka, R. C. and McDonough, W., Effect of stresses from thermal expansion anisotropy. Phase transformations, second phases on the strength of ceramics. *J. Am. Ceram. Soc.*, 1980, **63**, 703–710.
26. Krell, A., Teresiak, A. and Schlafer, D., Grain size dependent residual microstresses in sub-micron Al_2O_3 and ZrO_2 . *J. Eur. Ceram. Soc.*, 1996, **16**, 803–811.